

CIRCUIT MODEL SIMULATIONS FOR IONOSPHERIC PLASMA RESPONSE TO HIGH POTENTIAL SYSTEM

Hwang-Jae Rhee¹, W. John Raitt²

¹Radio Research Laboratory/Ministry of Information and Communication
Anyang, 431-082, Korea

²Center for Atmospheric and Space Sciences, Utah State University, U.S.A.
e-mail: rhee@cc.rri.go.kr

(Received Oct. 15, 1999; Accepted March 20, 2000)

ABSTRACT

When a deployed probe is biased by a high positive potential during a space experiment, the payload is induced to a negative voltage in order to balance the total current in the whole system. The return currents are due to the responding ions and secondary electrons on the payload surface. In order to understand the current collection mechanism, the process was simulated with a combination of resistor, inductor, and capacitor in SPICE program which was equivalent to the background plasma sheath. The simulation results were compared with experimental results from SPEAR-3 (Space Power Experiment Aboard Rocket-3). The return current curve in the simulation was compatible to the experimental result, and the simulation helped to predict the transient plasma response to a high voltage during the plasma sheath formation.

1. INTRODUCTION

Space experiments can provide the return current data by using a biased probe relative to the background plasma. Energetic charged particle emission to the background plasma leaves a charge imbalance having a net positive charge on the platform. Cooperative High Altitude Rocket Gun Experiments (CHARGE-2) was a tethered sounding rocket payload carrying an electron emission gun. This system was designed to investigate the electron interaction with ambient ionospheric plasma and the relation between the return current and the vehicle potential (Neubert et al. 1990, Myers et al. 1990).

A high-voltage bias can be introduced between separate parts of the vehicle using a local power supply (Myers et al. 1989). SPEAR-1 was designed to study the interaction of differentially biased high-potential electrodes with space plasma by using an internal power supply (Allred et al. 1988, Katz et al. 1989), instead of the electron beam emission used in CHARGE-2.

SPEAR-3 program was designed to study the interaction of a high-voltage system with the ambient ionospheric plasma at low earth orbit (LEO). The experiment intended to diagnose the relationship of the plasma current and applied potential, and to monitor the undisturbed and disturbed plasma and the neutral gas environments. The payload body was driven to a negative bias attracting ions while the positive sphere collected electrons, thereby achieving current balance for the system (Rhee et al. 1993, Rhee 1996).

This paper introduces an RLC circuit to simulate the plasma sheath which is formed around a biased electrode (Ma & Schunk 1989). The simulation with proper circuit in SPICE program finds the current signal which is similar to an actual response of the background plasma at the same environment of the SPEAR-3 experiment. This paper will show the way to set up the proper RLC circuit to confirm the experimental results, and to predict plasma responses to the applied potential in the experiment.

2. CIRCUIT MODEL AND SIMULATION

2.1. Instrumental Characteristics

To analyze the experimental result, and to set up the same situation to the simulation, it is necessary to understand the instrumental characteristics. High Speed Data System (HSDS) is connected to three channels to measure the current and potential of the spherical probe, and the current of the skin current monitoring system. The channel to the sphere current monitors the absorbed electron current on the sphere. The channel to the sphere potential measures the potential between the payload body and the spherical probe. The currents absorbed on the vehicle body are collected by the ion probe, and sampled by the HSDS. The HSDS employs an anti-aliasing low pass filter in each channel. The channel connected to the ion probe has a low pass filter whose cut-off frequency is 150 kHz, and the other two channels have 300-kHz cut-off low pass filters.

The 150-kHz low pass filter that is connected to the ion probe uses third-order Chebyshev polynomials. The transfer function of the low pass filter acquires 1.0 dB ripple Chebyshev polynomial in its denominator

$$H = \frac{G_{dc}(0.494)(0.994)}{(s+0.494)(s^2+0.494s+0.994)} \quad (1)$$

where G_{dc} is a gain constant, and s is the imaginary ratio of the input frequency to the cut-off frequency, $\omega_o = 9.42 \times 10^5$, corresponding to $f = 150$ kHz, $s = j\omega/\omega_o$. The parameters will be used in the Fourier transformation and inverse Fourier transformation for the simulation.

2.2 Equivalent Circuit Simulation in SPICE

Since Ma & Schunk (1989) shows that an RLC circuit is equivalent to the space plasma sheath around an electrode with a step voltage, equivalent RLC circuits to plasma sheaths are put into the circuit model in order to simulate the electron and ion sheaths around experimental system. A proper arrangement of capacitor, inductor, and resistor makes it possible to set up an equivalent circuit to the ion or electron current collection in each of the plasma sheaths. SPICE program, which is a general purpose circuit simulation program, is used for the simulation.

Steady-state currents and potentials provide the expected resistance to the resistor inside the sheath equivalent RLC circuit. The resistor is only the part to affect the steady-state current in the RLC circuit because, in a steady-state, the capacitor does not allow current to pass through on its discharging phase, and the inductor is no longer effective in decreasing current. Therefore, steady-state electron current and potential enable us to estimate the resistance in the electron sheath equivalent circuit. The measured steady-state current and potential of the probe are roughly 10^{-3} A and 10^3 V, respectively. Ohm's law gives $10^6 \Omega$ to the resistor of electron sheath equivalent RLC circuit.

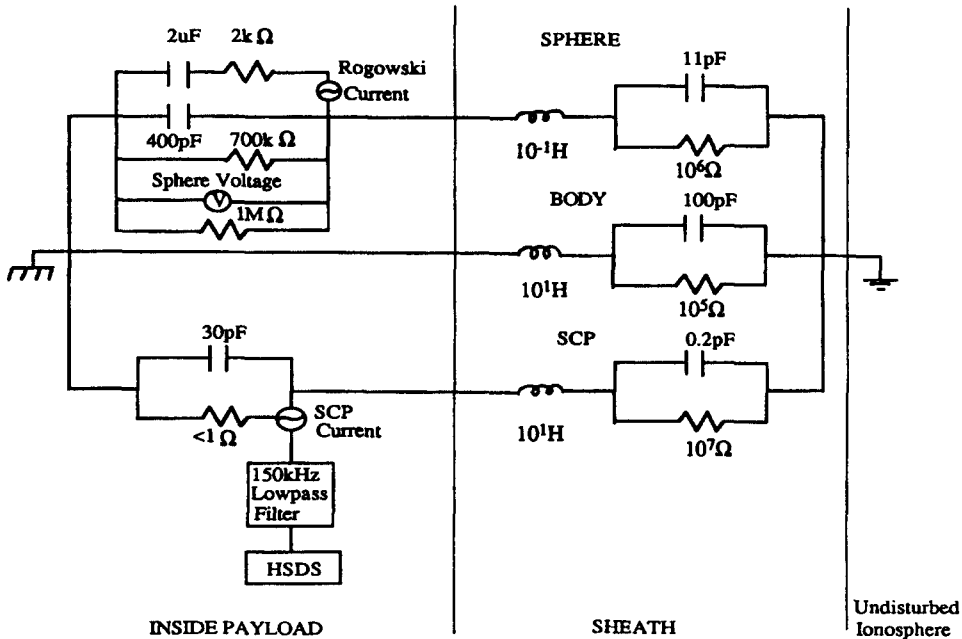


Figure 1. Simplified schematic diagram of the experimental system including sheath equivalent RLC circuits.

On the other hand, for the ion probe on the payload skin, it is possible to estimate the order of resistance from the steady-state current 10^{-5} A and potential 10^3 V. Ohm's law provides a resistance $10^7 \Omega$ to the resistor of the ion probe equivalent RLC circuit. Because the area of the payload body is approximately 600 times larger than the ion probe's, the return currents to the payload body are around 10^{-3} A, and the resistance is approximately $10^5 \Omega$.

The following equation gives the capacitance for a spherical electrode:

$$C_{sphere} = 4\pi\epsilon_0 \frac{ab}{b-a} \tag{2}$$

where C is the sphere's capacitor, a is the sphere radius, and b is the sheath radius. Calculated capacitance is 10 pF for a spherical probe whose radius is 0.1 m. A cylindrical electrode requires different expression for capacitance as shown in the equation (3)

$$C_{cylinder} = 2\pi\epsilon_0 \frac{L}{\ln(b/a)} \tag{3}$$

where L is the cylinder length, a is the cylinder radius, and b is the sheath radius. The expected capacitance of the payload body is approximately 100 pF because the estimated ion sheath radius is 10^0 m in the experimental environment and given vehicle potential, and the payload body length L and radius a are 5 m and 0.22 m, respectively.

The current damping coefficient is given by the ratio of resistance to inductance, R/L , in a parallel RLC circuit; the time constant of current decay is the inverse of the damping coefficient, L/R .

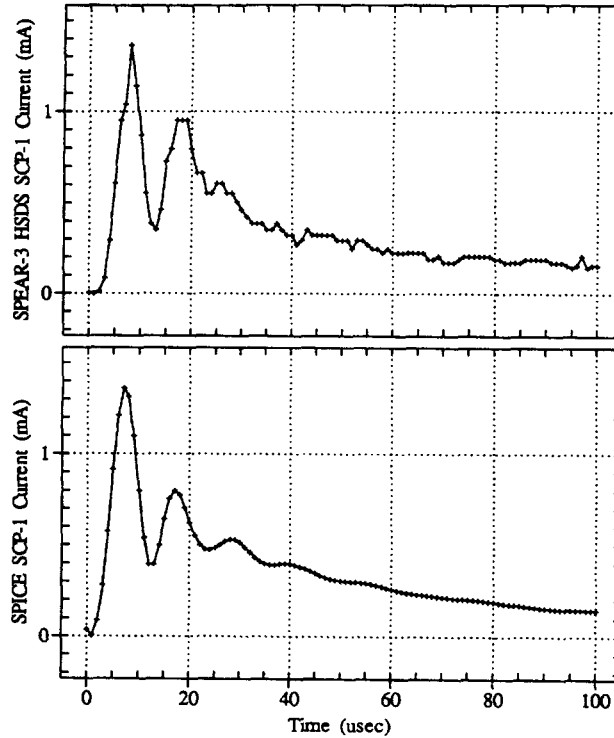


Figure 2. SPEAR-3 experimental plasma return current at altitude 289km (upper panel) and the simulated return current (lower panel).

The expected inductances are roughly 10^1 H in both the ion probe and vehicle body sheath equivalent circuits because the time constant of the ion current decay is approximately $50 \mu\text{sec}$, and the resistance is $10^5 \Omega$ in the vehicle body sheath equivalent circuit. In the electron sheath equivalent circuit, the expected inductance is 10^{-1} H because the inductance is proportional to the square root of the electron mass ratio to ion mass. Figure 1 shows the configuration of RLC circuits equivalent to the plasma sheaths which were formed around the experimental system.

In order to find out the simulation result in Figure 1, SPICE program adopts the resistances, capacitances, and inductances of the given RLC circuit where the orders are derived from the rough calculation explained above, and the optimum values from fittings of the simulation result. The simulation result will be shown in Figure 2.

3. RESULTS AND DISCUSSION

It is necessary to apply both the Fourier transformation and inverse Fourier transformation to the simulated ion current of the SPICE circuit because the experimental ion currents are filtered by the anti-aliasing low pass filter in the HSDS. Figure 2 shows the simulated ion currents in the SPICE model and the actual ion return current in the experiment. Each panel in the figure takes $100 \mu\text{sec}$ window on the x-axis, and the time resolution is $1 \mu\text{sec}$, which corresponds to the '+' sign in the

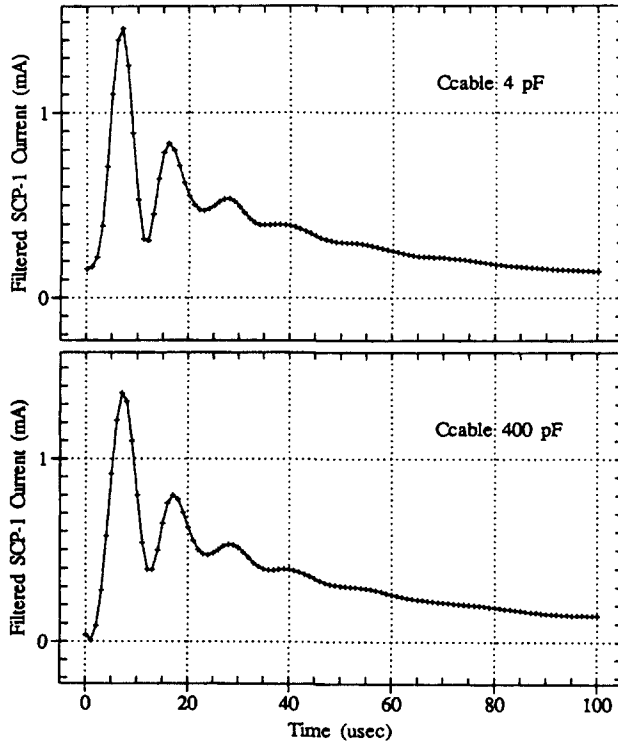


Figure 3. Comparison of the cable capacitance effect with two different capacitors of 4 pF (upper panel) and 400 pF (lower panel) in the SPICE simulation.

panels. The upper panel shows the ion current obtained from the experiment, and the lower panel presents the ion current of the SPICE circuit model. In the upper panel, the initial current peak occurs around $10 \mu\text{sec}$, and the current at the peak is approximately 1 mA. The second peak appears around $20 \mu\text{sec}$ so that the oscillation period of the ion current is about $10 \mu\text{sec}$. The SPICE simulation also shows that the oscillation period and current peak are close to those in the upper panel. After the second peak, the ion currents decay to the steady-state current in both the experiment and the simulation. The result presents that a proper set-up of the RLC circuits makes it possible to simulate the formation of plasma sheath around an electrode. However, in justification of the circuit model, it is needed to examine the capacitance effect due to the probe cable, and this will be checked in two ways in the simulation.

All of the capacitances, inductances and resistances are taken completely the same except the cable capacitance. For two different capacitors of 400 pF and 4 pF, Figure 3 shows a simulation result that the ion currents are almost the same in shape and magnitude, even though one of the cable capacitances is much less than the other. Therefore, because the cable capacitance does not affect the ion current, the simulated ion current in the SPICE model explains that the initial peak of the experimental ion current is not due to the instrumental capacitance effect.

The ion return current is due to the ions returning from the background plasma to the vehicle body. It is expected that the ion current is more sensitive to the vehicle body inductance than the

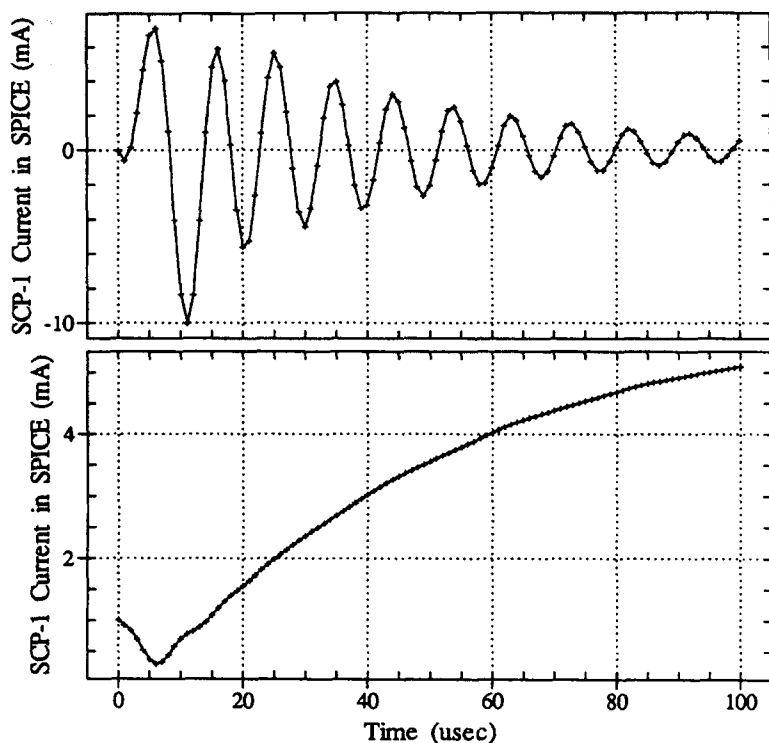


Figure 4. Simulated plasma return current for smaller (upper panel) and larger (lower panel) capacitance effect of the payload body.

electron probe inductance because ions are the main particles that produce the ion return current. Figure 4 shows a big difference between the ion return currents, as expected, when a smaller or larger capacitance is used in the ion sheath equivalent RLC circuit. On the other hand, compared with Figure 4, Figure 5 does not show any significant difference in the ion return current when a smaller or larger capacitance is used in the electron sheath equivalent RLC circuit.

Based on the above results, it is concluded that the peak of the experimental ion current is not due to the instrumental capacitance effect, but results from the ambient plasma characteristics because the cable capacitance does not affect the ion current in the simulation, and the current peaks are proportional to the RLC values in the sheath equivalent circuits.

4. SUMMARY AND CONCLUSION

The experimental results for the plasma return current were potentially deviated because the current monitoring system included anti-aliasing filter to transform the plasma reaction to the potential into current signal. The objective of the computer simulation for the plasma return current was to test the instrumental effect affecting on the signals, and to predict the transient return currents responding to a high potential. The simulation was performed in SPICE program with a combination of resistance, inductance, and capacitance in RLC circuit. Each factor in the RLC circuit was

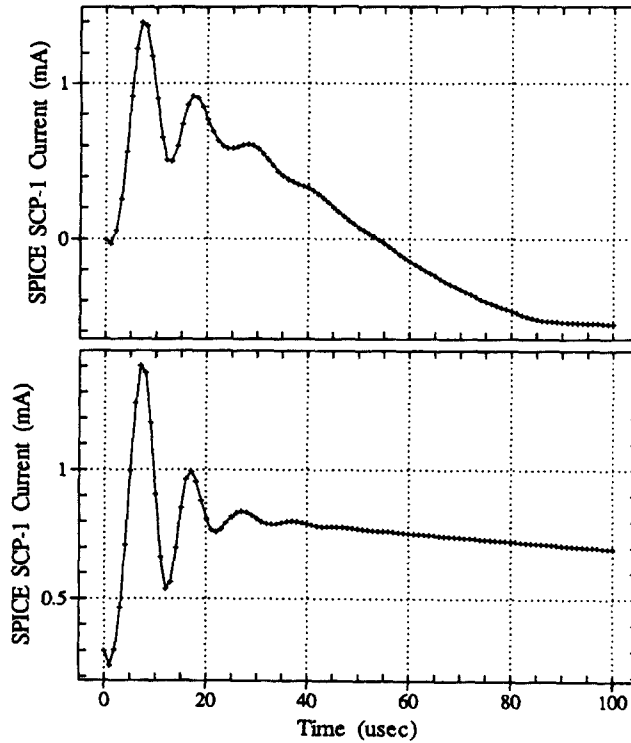


Figure 5. Simulated plasma return current for smaller (upper panel) and larger (lower panel) capacitance effect of the spherical probe.

selected according to the equivalent plasma sheath, and the circuit made it possible to simulate the return current collection in the experiment.

The circuit model showed that the anti-aliasing filter included in the current monitoring system did not affect the return current collection because the simulation results were consistent with the experimental results. This means that there was no deviation due to the effect of anti-aliasing filter installed in the instrument, and the plasma current from the current monitoring system could be considered as a real plasma reaction to the applied potential.

In addition, the simulation showed that if an appropriate RLC circuit model in SPICE program was used, the simulation can predict an actual response of plasma current for a given potential and electrode. The effective factors were the level of steady-state current, damping rate of the reacted plasma current, dimension of electrode, and the environmental values in actual situation. Therefore, the RLC circuit model will be effectively used to predict plasma response once we determine the effective factors and the associated RLC factor values.

REFERENCES

Allred, D. B., Benson, J. D., Cohen, H. A., Raitt, W. J., Burt, D. A., Katz, I., Jongeward, G., Alport, M. J., Antoniadis, J. A., Boyd, D. A., Nunnally, W. C., Dillon, W. E., Picket, J., & Torbert,

- R. B. 1988, *IEEE Trans. Nuclear Sci.*, 35, 1386
- Katz, I., Jongeward, G. A., Davis, V. A., Mandell, M. J., Kuharski, R. A., Lilley, J. R., Jr., Raitt, W. J., Cooke, D. L., Torbert, R. B., Larson, G., & Rau, D. J. 1989, *Geophys. Res.*, 94, 1450
- Ma, T.-Z., & Schunk, R. W. 1989, *Plasma Phys. and Controlled Fusion*, 31, 399
- Myers, N. B., Raitt, W. J., Gilchrist, B. E., Banks, P. M., Neubert, T., Williamson, P. R., & Sasaki, S. 1989, *Geophys. Res. Lett.*, 16, 365
- Myers, N. B., Raitt, W. J., White, A. B., Banks, P. M., Gilchrist, B. E., & Sasaki, S. 1990, *J. Spacecr. Rockets*, 27, 25
- Neubert, T., Mandell, M. J., Sasaki, S., Gilchrist, B. E., Banks, P. M., Williamson, P. R., Raitt, W. J., Meyers, N. B., Oyama, K. I., & Katz, I. 1990, *J. Geophys. Res.*, 95, 6155
- Rhee, H.-J. 1996, *JA&SS*, 13, 206
- Rhee, H.-J., Berg, G. A., & Raitt, W. J. 1993, *EOS Trans AGU*, 74, 468